Radio and millimeter observations of z $\sim$ 2 luminous QSOs

A. O. Petric

Astronomy Department, Columbia University, New York, NY USA
andreea@astro.columbia.edu

C. L. Carilli

National Radio Astronomy Observatory, P.O. Box O, Socorro, NM, 87801, USA
ccarilli@nrao.edu

F. Bertoldi

Argelander Institute für Astronomie, Universität Bonn, Auf dem Hügel 71, 5321 Bonn, Germany

A. Beelen

Max-Plank-Institut fur Radioastronomie, Auf dem Hügel 69, 53121 Bonn, Germany

P. Cox

IRAM, 300 rue de la Piscine, Domaine Universitaire, F-38406 Saint Martin d'Heres, France

A. Omont

Institute d'Astrophysique de Paris, CNRS, 98bis boulevard Arago, 75014 Paris, France

ABSTRACT

We present Very Large Array observations at 1.4 and 5 GHz of a sample of 16 quasi-stellar objects (QSOs) at $z = 1.78$ to 2.71. Half of the chosen quasars are bright at mm wavelengths (250 or 350 GHz) while the other half were not detected at mm wavelengths; the former QSOs were detected at 1.4 GHz, in most cases at high significance (S/N $\geq$ 7), but only three of the latter sources were detected at radio frequencies, and only at lower significance (S/N $\sim$ 3). The data are consistent with a correlation between the mm and radio fluxes indicating a physical connection between the mechanisms responsible for the radio and mm emission. However, this conclusion is based on data including many upper limits, and deeper data are clearly needed to verify this correlation.

All eight mm detected QSOs are detected in the radio continuum, with radio flux densities consistent with the radio-to-FIR correlation for low z star forming galaxies. However, four of these have flatter spectral indices than is typical for star forming galaxies (i.e. greater than -0.5) suggesting that radiation from the central AGN dominates the observed radio emission. All the sources detected at 1.4 GHz are spatially unresolved, with the size limits typically $< 1'' = 6$ kpc. High star formation rate galaxies at low redshift are typically nuclear starbursts, with sizes < 1 kpc. Hence, the current radio size limits are insufficient to constrain the emission model (AGN or starburst).

Subject headings: dust: QSOs, galaxies — radio continuum: QSOs, galaxies — infrared: QSOs, galaxies — galaxies: starburst, evolution, active

1. Introduction

Studies of the dynamics of stars and gas in the nuclear regions of nearby galaxies suggest that the vast majority of spheroidal galaxies in the nearby universe contain massive black holes and that the mass of the central black holes correlates with the velocity dispersion in the spheroid (Magorrian et al. 1998, Ferrarese & Merritt 2000, Gebhardt et al. 2000, Tremaine et al. 2002). These findings suggest a fundamental relationship between the formation of massive black holes and the stellar content of galaxies. Radio-millimeter studies of ($z > 2$) QSO's indicate that about 20–30% of the sources are detected in surveys with 3 σ flux density limits of 1.5 to 4 mJy at 250 GHz (Omont et al. 2001, 2003; Carilli et al. 2001a,b; Isaak et al. 2002, Bertoldi et al. 2003a,b, Petric et al. 2003, Beelen et al. 2006). The mm-to-cm spectral indices of these sources imply that the mm radiation is thermal emission from warm dust, and that in many of the sources the spectra are consistent with the dust being heated by star formation (Carilli et al. 2001b). Detections of CO line emission from FIR luminous QSOs indicated the presence of large gas reservoirs ($\sim 10^{11} M_\odot$; Cox et al. 2002, Walter et al. 2003), leading some authors to conclude that active star formation is inevitable (Omont et al. 2001).

However, the issue of what heats the dust in dusty IR bright QSOs has not been settled. Chini, Kreysa, & Biermann (1989) found that most z < 0.4 QSOs show dust emission with dust masses about a few times 10^7 $M_\odot$. On the basis of mm to X-ray spectral indices, these authors argue that the dominant dust heating mechanism is radiation from the AGN. Benford et al. (1999) analyze a sample of 20 mostly radio quiet quasars with redshifts between 1.8 and 4.7 by combining their measurements at 350 microns with data from other far-infrared and millimeter wavelengths. These authors try to fit the spectral energy distribution and

find that the SEDs are consistent with the FIR luminosity being dominated by emission from a dust component at $\sim$ 50K. This is similar to what is found for ultraluminous infrared galaxies, however for the majority of sources in their sample a large luminosity contribution from higher temperature dust cannot be ruled out. Haas et al. (2000, 2003) obtain infrared to millimeter spectral energy distributions for a random sample of Palomar Green quasars and learn that the SEDs show a variety of shapes (power-law, mid-infrared dominated, and far-infrared dominated). This suggests that more than one type of source or heating mechanism or dust are responsible for the obseved SEDs.

A detailed far-IR photometry study of a sample of optically selected bright quasars done by Andreani et al. (2003) does not find a strong connection between the B luminosity and the warm dust color temperature and thus suggest that there is no strong relation between the energy emitted by the nuclear source and that emitted in the FIR. McMahon et al. (1994), Isaak et al. (2002), Omont et al. (2001), (2003) find no connection between absolute luminosity and mm/submm flux (see however, Beelen et al. in preparation for evidence of a mild correlation). In particular it should be stressed that the sources of Table 1 are exceptional both for their UV and FIR luminosity. Even if the detailed quantitative correlation between L_{FIR} and L_{bol} is weak in the luminosity range considered, the overall probability to have an hyperluminous starburst ($L_{FIR} > 10^{13}$ $L_{\odot}$) in such hyperluminous high z QSOs is high at more than 30%. Such a correlation does not necessarily imply that the FIR emission is heated by the AGN since the M_{BH}/σ Magorrian et al. (1998) relation would also argue for a correlation in objects where the black hole and starburst are growing coevally. The exceptional FIR luminosity of such QSOs is also consistent with the rapidly developing 'feedback' models aimed at explaining the M_{BH}/σ relation (see e.g. Springel et al. 2005, Hopkins et al. 2005 and references therein), as well as with parallel submm results on X-ray absorbed QSOs (Page et al. 2004) which show a gross correlation between feeding the QSO and the starburst with interstellar gas.

These results seem to fit in with a picture in which the emission is only loosely related to the detailed physics of the surrounding medium and so argues in favor of linking the FIR to a concurrent starburst. Page et al. (2001, see also Page et al. 2004) use submillimeter photometry of eight X-ray-absorbed AGN, to argue that the AGN are not sufficiently powerful to heat the FIR emitting dust, but that the FIR is predominantly powered by starlight rather than the central AGN. Similarly, Alexander et al. (2004,2005a,b), observed a population of submm SCUBA sources combining ultra-deep X-ray observations and deep optical spectroscopic data. These authors found that a significant fraction ($\geq$ 38%) of the brightest (i.e. 350 GHz flux densities greater than 5mJy) SCUBA galaxies do harbor AGNs; but in almost all cases star formation dominates their bolometric luminosity.

This paper presents the radio (1.4 and 5 GHz) continuum properties of a sample of 16 QSOs at z $\sim$ 2. These sources were chosen to (1) have similar optical properties (M_B, spectra) to those of quasar samples with redshifts greater than 3.7 for which we have comparable (sub)millimeter and centimeter observations and (2) be radio quiet, that is not detected in the Faint Images of the Radio Sky at Twenty-Centimeter (FIRST) survey which has a typical sensitivity limit of $\sigma = 0.15$ mJy (Becker, White, & Helfand 1995). Half of the observed quasars are bright at 250 GHz ($S_{250} \gtrsim$ $\sim$4 mJy, Omont et al. 2003) or 350 GHz ($S_{350} \gtrsim$ $\sim$10 mJy, Priddey et al. 2003) (Table 1) which implies $L_{FIR} > 10^{13} L_{\odot}$, and the other half have not been detected at either of these frequencies. These data help constrain the evolution with redshift of the radio-to-optical SEDs of luminous QSOs. We also look for systematic differences between the radio properties of FIR bright and FIR faint quasars, and examine evidence for star formation in these systems. We use $\Omega_{\rm M} = 0.3$, $\Omega_{\lambda} = 0.7$ and $H_0 = 71$ km s^{-1}. For comparison with previous work (e.g. Omont et. al 2003) we also give the alternative M_B magnitudes in an Einstein - de Sitter (EdS) cosmology, $\Omega_{\rm M} = 1.0$, $\Omega_{\lambda} = 0$ and $H_0 = 50$ km s^{-1}

2. Observations

VLA observations at 1.4 GHz were made on April 2002, in the A configuration (max. baseline = 30 km), with a total bandwidth of 100 MHz and two orthogonal polarizations. Each source was observed for about one hour at 1.4 GHz. Standard phase and amplitude calibration was applied, and all sources were self-calibrated using field sources. The absolute flux density scale was set with observations of either 3C48 or 3C286.

The final images were generated using the wide field imaging (Cotton 1999; Bridle & Schwab 1999) and deconvolution capabilities of the Astronomical Image Processing System task IMAGR. The theoretical rms noise (σ) value corresponding to 1 hour of observing in continuum mode at 1.4 GHz is 23 μJy, and in most of the maps presented here this sensitivity is roughly achieved. The Gaussian restoring CLEAN beam Full Width at Half Maximum (FWHM) was typically $\sim 1\farcs5$ for the A configuration observations.

The eight FIR-bright sources were observed at 5 GHz on October, 2002 in C configuration for $\sim$ 20 minutes, achieving an rms sensitivity of order 45 μJy. The Gaussian restoring CLEAN beam FWHM was typically of order $4''$ for the C configuration observations. The lower quality of the 5GHz data did not permit an appropriate fit to determine the source size. When determining the spectral indices we used the integrated 5 GHz fluxes and their respective errors.

The 250 GHz data, used in the analysis for this paper, were obtained with the Max-Planck Milimeter Bolometer (MAMBO) array (Kreysa et al. 1999) at the IRAM 30m telescope on Pico Veleta in Spain with 1 σ flux density sensitivities ranging between 0.6 and 1.3 mJy; and are described in detail in Omont et al. (2003).

3. Results and Analysis

The results for the mm-detected quasars are presented in the upper half of Table 1, while those for the mm-non-detected sources are given in the lower half. The 250 GHz data are described by Omont et al. (2003), while the 350 GHz properties of J0018-0220 and J0035+4405 are detailed by Priddey et al. (2003).

When considering radio emission from the target sources, an important issue is astrometry and source confusion. The positional uncertainty for the radio observations is given by: $\sigma_\theta \sim \frac{FWHM}{SNR}$ (Fomalont 1999), where FWHM corresponds to that of the Gaussian restoring beam, and SNR=Signal-to-Noise ratio of the detection. For a 3σ detection this corresponds to $0\farcs5$ for most of our sources. To this must be added the typical astrometric uncertainty of the optical data, and the uncertainty in the relationship between radio and optical reference frame which is about $0\farcs25$ (Deutsch 1999). Considering confusion, Fomalont (2006, in prep.) show that the sub-mJy source counts follow the relation: $N(> S_{1.4}) = 0.026 \times S_{1.4}^{-1.1}$ arcmin^{-2}, with 1.4 GHz flux density, $S_{1.4}$, in mJy. Hence, within $1\farcs5$ of a given source we expect 6×10^{-4} sources with $S_{1.4} \geq 70$ μJy by chance. A deep survey of 357 square arcminutes by Greve et al. (2004) find that there are 15 sources in the region surveyed with $S_{250} > 3.75$ mJy. At this flux density level we expect about 0.003 sources by chance within the beam of the 30m telescope (i.e. within $5''$ of the target source). Overall, we only consider radio emission as associated with the QSO if it is $> 3\sigma$ and located within $1\farcs5$ of its given optical position.

Using these criteria, all of the mm-detected sources are also detected at 1.4 GHz with flux densities between 0.14 and 0.94 mJy. Moreover, in all but one case, the sources are detected at high significance ($> 7\sigma$). Conversely, only three of the mm-non-detected sources are detected at 1.4 GHz, and all of these are fainter than 0.17 mJy.

The 1.4 GHz images of the detected sources are shown in Figure 1. The optical positions are indicated by crosses. From Gaussian fitting we find no clear evidence that any of the sources are extended at the 1.4 GHz resolution of $\sim 1\farcs5$, with typical upper limits to source sizes of $\sim 1''$. The 4.8 GHz images of the detected sources are shown in Figure 2.

4. The radio-FIR correlation

In the local universe star-forming galaxies from optically, IR or radio selected samples follow a very tight linear relation between their radio continuum and FIR luminosities, with only a factor of two scatter around linearity over four orders of magnitude in luminosity (Condon 1992; Condon & Yin 1990; Miller & Owen 2001; Yun, Reddy, & Condon 2001). If this correlation holds at high redshift (Carilli & Yun 1999; 2000; Yun & Carilli 2002; Elbaz et al. 2002, Appleton et al. 2004) then the ratio of radio to FIR fluxes can be used to constrain the star formation properties of high z QSOs. Recent work by Chapman et al. (2005) suggests that the radio-FIR correlation also holds in the case of submillimeter galaxies with redshifts between 1.7 and 3.6. These authors use the 850μm and radio data with the spectroscopic redshift, to estimate dust temperatures for the sources in their sample. This is done by assuming a spectral energy distribution (SED) like that of an object which would fall on the FIR-radio correlation. Chapman et al. (2005) also observe a subset of these galaxies at 450μm to confirm the determined temperatures and SEDs, and so vindicates the assumption that the FIR-radio correlation can be used to estimate star formation rates in their sample.

However, an important caveat is that lower luminosity, radio quiet QSOs at lower redshift also follow the standard radio–FIR correlation for star forming galaxies (Sopp & Alexander 1991). This can also be seen in the Haas et al. (2003) sample of PG QSOs. It is unclear whether the sources in the Sopp & Alexander sample also host significant active star formation. Overall, whether or not an object is on the radio-FIR trend is only a consistency check that the source is actively forming stars, but certainly not conclusive proof thereof. Therefore, it ought to be used in conjunction with at least one other star formation diagnostic such as radio spectral index, variability or source size.

The radio to FIR correlation is typically quantified through the parameter q defined as:

$$q \;=\; \log\left(\frac{\mathrm{L_{FIR}}}{3.75 \;\times\; 10^{12}\ \mathrm{Wm^{-2}}}\right) \;-\; \log\left(\frac{\mathrm{F_{1.4}}}{\mathrm{Wm^{-2}Hz^{-1}}}\right)$$

where $L_{\rm FIR}$ corresponds to the FIR luminosity between 40 and 120 μm and $F_{1.4}$ is the radio flux at 1.4 GHz in W m^{-2} Hz^{-1}. In their extensive study of 2000 IRAS-selected galaxies, Yun, Reddy & Condon (2001) find a mean q value of 2.34, and that 98% of these sources are within $\pm$ log(5) of the mean. They conclude that this range (q = 1.64 to 3) corresponds to star forming galaxies, while significantly lower q values imply a contribution from a radio-loud AGN.

A second star formation diagnostic is the radio spectral index, with a typical value of $\alpha \sim -0.75 \pm 0.25$ for star forming galaxies (Condon 1992). Sub-arcsecond scale radio

emission from high z AGN is typically flat spectrum ($\alpha \sim 0$), although there are exceptions, namely compact steep spectrum sources (CSOs; O'Dea 1998). Given the existence of CSOs, we consider the radio spectral index an additional consistency check for star formation.

Table 2 presents some of the estimated parameters for these sources (names of in Column [1]) which were detected in FIR. Their bolometric luminosities (Column [2]) were estimated from the absolute blue magnitudes given by Omont et al. (2003), using a WMAP cosmology. Omont et al. (2003) used the standard Einstein-de Sitter cosmology with $H_0 = 50$ km s^{-1} Mpc^{-1}, and $q_0 = 0.5$ to estimate the rest-frame absolute B band magnitudes, and so we scaled the blue magnitudes to the concordance cosmology by scaling the luminosity distances accordingly. To convert the blue luminosity $L_{\rm B}$ to a bolometric measurement $L_{\rm bol}$ we assumed a bolometric correction from the B band of $L_{\rm bol}/L_{\rm B} = 12$ (Elvis et al. 1994). The radio properties such as the rest frame luminosity at 1.4 GHz and 5 to 1.4 GHz radio spectral indices are shown in columns [3] and [4]. For consistency with earlier treatments (Omont et al. 2001, 2003) the FIR luminosity (column [5]) was derived assuming a dust temperature and dust emissivity of 45 K and an emissivity index $\beta = 1.5$ which, in this redshift range, translates to the following scaling: $L_{\rm FIR} = 4.7 \times 10^{12} (\frac{Dl_{H_0=65}}{Dl_{H_0=71}})^2 (\frac{S_{250}}{\rm mJy})$ L$_\odot$, where $Dl_{H_0=65}$ and $Dl_{H_0=71}$ are the luminosity distances for the cosmologies used in Omont (2003) and this paper.[1] The q parameter is given in column [6].

5. Discussion

We find a very clear relationship between the mm and radio emission properties for the quasars in our sample. Although all the mm-detected sources are also detected at 1.4 GHz, in all cases the 1.4 GHz flux density is much less than the 250 GHz flux density, typically by an order of magnitude or more. Such a sharply rising spectrum from the radio through the (rest frame) FIR is good evidence for the FIR emission being thermal emission from warm dust (Carilli et al. 2002), as has been confirmed through multi frequency (rest frame) FIR observations of selected sources, including some of the sources in the current sample (Benford et al. 1999; Beelen et al. 2006).

An important issue concerning the mm fluxes of high z QSOs is whether there is a continuum of mm luminosities, or whether there are two physically distinct types of QSOs – mm-loud and mm-quiet. The flux limits on the non-detections in current mm and submm studies allow for either possibility. However, Bertoldi et al. (in preparation) suggest that the average of non-detections yields a clear detection, and that the distribution of flux densities

[1]The FIR properties of these sources are discussed in detail in Omont et al. 2003

can be fit by an exponential. On the other hand, submm observations of a sample of X-ray absorbed and non-absorbed AGN find that strong submillimeter emission is found only in X-ray absorbed sources (Page et al. 2004, 2001).

The radio observations presented herein are interesting in this regard. All eight mm-loud sources in our study were detected at 1.4 GHz, and all but one of these at high significance ($\geq 0.2 \pm 0.02$ mJy). Only three of the eight mm-quiet QSO's were detected at 1.4 GHz, and these at lower flux densities (≤ 0.17 mJy), and the rest were not detected in images with rms values ~ 0.02 mJy. Recall that all the sources were selected to have similar optical magnitudes, such that the radio and mm differences are unlikely to relate to differences in bolometric luminosity or magnification by gravitational lensing. We performed a statistical study based on methods which take upper limits formally into account, using the statistics package ASURV (Fiegelson & Nelson (1985), Isobe et al. (1986)). The statistical tests used indicate that the two populations are different to a high significance level, that is the probability that, based on their radio properties at 1.4 GHz, the two samples of submm-detected and non-detected quasars are drawn from the same population is very low —($\sim 10^{-4}$).

Figure 3 shows that a simple explanation for the different 1.4 GHz flux density distributions for the submm detected versus non-detected sources may be a correlation between the 1.4 GHz and FIR luminosities for QSO host galaxies. In Figure 3 we show that the 1.4 GHz and FIR luminosities of the sources (including limits), are consistent with a correlation between the two bands. This suggests a connection between the mechanisms producing the emission in each band. Such a connection would be a natural consequence of star formation. We note that flux density is not proportional to redshift so this tentative correlation cannot result from a mutual correlation with distance.

However, our samples are very small so it is difficult to ascertain what factors are responsible for the lower level of activity in the non-FIR detected sources. Clearly, more sensitive surveys of QSOs at multiple wavelengths are required to properly test the hypothesis that there are two physically distinct populations of mm-loud and mm-quiet sources and to understand the evolutionary stage of these sources.

As shown in Figure 4, all of the eight mm detected QSOs are detected in the radio continuum, with radio flux densities consistent with the radio-to-FIR correlation for low z star forming galaxies. However, four of these have flatter spectral indices than is typical for star forming galaxies ($\alpha^5_{1.4} > -0.5$).

The other four mm-detected sources are either at the low end of the q range defined for star forming galaxies, or have flat radio spectral indices (Table 2). It is possible that very

early in its evolution ($\leq 10^6$ years), ie. before many supernovae have populated the ISM with cosmic ray electrons, a starburst may show a flat spectral index, corresponding to free-free radio emission. A flat index may be seen if we were observing a very young starburst, in which the thermal free-free emission from O and B stars overwhelms the synchrotron from SNe. However this scenario would imply that we are looking at this object during a rapid and massive starburst. It seems more likely that in the sources with flat radio indices, the radiation from the central AGN dominates the observed radio emission.

J0018-0220, J0812+4028, J1409+5628 and J1611+4719, satisfy both the spectral index and q parameter criteria for star forming galaxies, although we re-emphasize neither test is definitive in this regard. If the dust is heated by star formation, the implied star formation rates are of order 10^3 $M_\odot$ year^{-1} (Omont et al. 2003). At this rate, assuming a Salpeter IMF, a large fraction of the stars in the host spheroidal galaxy could form on a typical dynamical timescale of 10^7 to 10^8 years. For one source, J1409+5628, a massive reservoir of molecular gas ($\sim 10^{11}$ $M_\odot$), the required fuel for such a starburst, has recently been detected (Beelen et al. 2004). Similar searches are underway for CO emission from the other QSOs.

All the sources detected at 1.4 GHz are spatially unresolved, with the size limits typically $< 1'' = 6$ kpc. High star formation rate galaxies at low redshift are typically nuclear starbursts, with sizes < 1 kpc. Hence, the current radio size limits are insufficient to constrain the emission model (AGN or starburst). A potentially powerful test of AGN vs. starburst radio emission comes from VLBI observations, to search for extended (on scales of 100's of pc), lower surface brightness radio emission. Recent VLBI observations (Momjian, Petric & Carilli 2004, Momjian, Carilli, & Petric 2005) of one of the sources in our sample (J1409+5628), show extended emission on scales of 100 pc with an intrinsic brightness temperatures $< 10^5$ K at 8 GHz, as expected for a starburst nucleus (Condon & Yin 1990), and inconsistent with a radio-jet source (CSO or core-jet; Beelen et al. 2004).

CC would like to acknowledge support from the Max-Planck-Forschungspreis. The National Radio Astronomy Observatory (NRAO) is a facility of the National Science Foundation, operated under cooperative agreement by Associated Universities, Inc. We also thank an anonymous referee that helped improve the structure and content of this paper.

REFERENCES

Alexander, D.M., 2004, astroph-0401129; in *Multiwavelength Mapping of Galaxy Formation and Evolution*, R. Bender & A. Renzini (eds), ESOUSM/MPE workshop-proceedings

Alexander, D.M., et al. 2005a, Nature, 434, 738

Alexander, D.M., et al. 2005b, ApJ, 632, 736

Andreani, P., Cristiani, S., Grazian, A., La Franca, F., & Goldschmidt, P. 2003, AJ 125, 444

Appleton, P.N., Fadda, D.T., Marleau, F.R., Frayer, D.T. et al. 2004, ApJS, 154,147

Becker, R. H., White, R. L., & Helfand, D. J. 1995, ApJ, 450, 559

Beelen,A., Cox,P., Benford, D.J.,, Dowell,C.D., et al. 2006, ApJ, in press: astroph0603121

Benford, D.J., Cox, P., Omont, A., Phillips, T. G., & McMahon, R. G.,1999, ApJ, 518, L65

Bertoldi, F., Carilli, C. L., Cox, P., Fan, X., et al. 2003a, A&A, 406, 55

Bertoldi, F., Cox, P., Neri, R., Carilli., C.L., et al. 2003b, A&A., 409, 4

Beelen, A., Cox, P., Pety, J., Carilli, C.L., et al. 2004, A&A, 423, 441

Bridle, A.H., & Schwab, F.R. 1999, in ASP Conf. Ser. 180, Bandwidth and Time-Average Smearing in Synthesis Imaging in Radio Astronomy II, ed. G.B.Taylor, C.L. Carilli, & R. A. Perley (San Francisco: ASP), 357

Carilli, C.L., Bertoldi, F., Omont, A., Cox, P. et al. 2001a, AJ, 122, 1679

Carilli, C.L., Bertoldi, F., Rupen, M.P., Fan, X., et al. 2001b, ApJ, 555, 625

Carilli, C.L., Cox, P., Bertoldi, F., Menten, K.M, et al. 2002, ApJ, 575, 145

Carilli, C.L., & Yun, M.S., 1999, ApJ, 513, 13

Carilli, C.L., Yun, M.S., 2000, ApJ, 530, 618

Chapman, S.C., Blain, A. W., Smail, I, Ivison, R. J. 2005, ApJ, 622, 772

Chini, R., Kreysa, E., Biermann, P.L., 1989, A&A, 219, 87

Condon, J.J. 1992, ARA&A, 30, 575

Condon, J.J. & Yin, Z.F. 1990, ApJ 357, 97

Cotton, W. D. 1999, in ASP Conf. Ser. 180, Synthesis Imaging in Radio Astronomy II, ed. G.B.Taylor, C.L. Carilli, & R. A. Perley (San Francisco: ASP), 357

Cox, P., Omont, A., Djorgovsky, S.G., Bertoldi, F., et al. 2002, A&A 387, 406

Deutsch, E.W. 1999, AJ, 118, 1882

Elbaz, D., Cesarsky, C. J., Chanial, P., Aussel, H., et al. 2002, A&A 284, 848

Elvis, M., Wilkes, B. J., McDowel, J.C., Green, R.F.,. et al. 1994, ApJS, 95, 1

Feigelson, E. D., & Nelson, P. I.1985, ApJ, 293, 192

Fomalont, E.B., 1999, in ASP Conf. Ser. 180, Bandwidth and Time-Average Smearing in Synthesis Imaging in Radio Astronomy II, ed. G.B.Taylor, C.L. Carilli, & R. A. Perley (San Francisco: ASP), 35

Ferrarese, L., & Merritt, D. 2000, ApJ, 539, L9

Gebhardt, K., Kormendy, J., Ho, L., Bender, R., et al. 2000, ApJ, 543, L5

Greve, T.R., Ivison, R.J., Bertoldi, F., Stevens, J.A., et al. 2004, MNRAS 354, 779

Haas, M., , Muller, S.A.H., Chini., R., Meisenheimer, K., et al. 2000, A&A 354, 45

Haas, M., Klaas, U., Müller, S.,A., Bertoldi, F., et al. 2003, A&A 402, 87

Hopkins, P.F., Hernquist, L. Cox, L., et al. 2005, submitted to ApJ, astroph/05036398

Isaak, K.G., Priddey, R.S., McMahon, R.G., Omont., A., et al., 2002, MNRAS, 329, 149I

Isobe, T., Feigelson, E.D., & Nelson, P. I., 1986, ApJ, 306, 490

Kreysa, E., et al. 1998, Proc. SPIE, 3357, 319

Magorrian, J., Tremaine, S., Richstone, D., Bender, R., et al. 1998, AJ, 115, 2285

McMahon, R.G., Omont, A., Bergeron, J., Kreysa, E., & Haslam, C.G.T., 1994, MNRAS, 267

Miller, N.A., & Owen, F.N., 2001, AJ, 121

Momjian, E., Petric, A., & Carilli, C. L., 2004, AJ, 127, 587

Momjian, E., Carilli, C.L., & Petric, A.O., 2005, AJ 129, 1809

O'Dea, C.P. 1998, PASP, 110, 493

Omont, A., Beelen, A., Bertoldi, F. et al. 2003, A&A, 398, 857

Omont, A., Cox., P., Bertoldi, F., McMahon, R.G., 2001, A&A., 374, 371

Page, M.J., 2001, MNRAS, 325, 575

Page, M.J., Stevens, J.A., Mittaz, J.P.D., Carrera, F.J., 2001, Science 294, 2516

Page, M.J., Stevens, J.A., Ivison, R.J., Carrera, F.J., 2004,ApJ, 611, L85

Petric, A.O., Carilli, C.L., Bertoldi, F., Fan, X., et al. 2003, AJ 126, 15

Priddey, R. S., Isaak, K. G., McMahon, R. G., & Omont, A., 2003, MNRAS, 339, 1183

Springel, V., Di Matteo, T., & Hernquist, L. 2005, ApJ 620, 79

Sopp, H. & Alexander, P., 1991, MNRAS, 251P, 14

Tremaine, S., Gebhardt, K., Bender, R., Bower, G., et al. 2002, ApJ, 574, 740

Walter, F., Bertoldi, F., Carilli, C.L., Cox, P., et al. 2003, Nature, 424, 406

Yun, M.S., Reddy, N.A., & Condon, J.J., 2001, ApJ, 554, 803

Yun,M. S., & Carilli, C. L., 2002, ApJ, 568, 88

Table 1. Observed Properties

QSO	z	M_B^{λ} (M_B ^{EdS})	Optical Position (J2000) RA (h m d)	DEC (° ′ ″)	Radio 1.4 GHz Position (J2000) RA (h m d)	DEC (° ′ ″)	$S_{1.4}$ [1.0e-6 Jy]	$S_{5.0}$ [1.0e-6 Jy]	S_{250} [1.0e-3 Jy]
Properties of sources detected in mm/mm									
J0018-0220	2.56	-28.4(-28.3)	00 21 27.37	-02 03 33.8	00 21 27.24	-02 03 33.6	260 ± 20	<120	**[a]
J0035+4405	2.71	-28.5(-28.4)	00 37 52.31	44 21 32.9	00 37 52.33	44 21 32.9	150 ± 16	< 120	**[b]
J0812+4028	1.78	-27.0(-27.0)	08 12 00.50	40 28 14.0	08 12 00.50	40 28 14.3	200 ± 60	< 100	4.3± 0.8[c]
J0937+7301	2.52	-28.6(-28.5)	09 37 48.89	73 01 58.3[d]	09 37 48.89	73 01 58.1	440 ± 20	530 ± 36	3.8± 0.9[c]
J1409+5628	2.56	-28.5(-28.4)	14 09 55.60	56 28 26.2[d]	14 09 55.57	56 28 26.5	940 ± 20	310 ± 60	10.7± 0.6[c]
J1543+5359	2.37	-28.4(-28.3)	15 43 59.37	53 59 03.1[d]	15 43 59.45	53 59 03.3	140 ± 20	370 ± 100	3.8± 0.9[c]
J1611+4719	2.35	-27.8(-27.7)	16 12 39.90	47 11 58.0	16 12 39.91	47 11 57.6	200 ± 20	< 120	4.6± 7[c]
J1649+5303	2.26	-28.2(-28.2)	16 49 15.02	53 03 16.5[d]	16 49 15.00	53 03 16.6	820 ± 20	910 ± 80	4.6± 0.8[c]
Properties of sources with mm/mm upper limits									
J0837+145	2.51	-28.2(-28.1)	08 37 12.60	14 59 17.0	...	...	<81	...	< 1.8[c]
J0958+470	2.48	-27.8(-27.7)	09 58 45.50	47 03 24.0	...	...	<81	...	< 2.1[c]
J0914+582	1.95	-27.1(-27.1)	09 14 25.80	58 25 19.0	09 14 25.74	58 25 19.4	120 ± 31	...	< 1.8[c]
J1210+3939	2.40	-27.8(-27.7)	12 10 10.20	39 39 36.0	12 10 10.22	39 39 35.7	74 ± 24	...	< 2.4[c]
J1304+2953	2.85	-28.1(-28.0)	13 04 12.00	29 53 49.0	13 04 11.97	29 53 49.1	88 ± 22	...	< 3.0[c]
J1309+2814	2.21	-27.9(-27.9)	13 09 17.20	28 14 04.0	...	...	<66	...	< 3.0[c]
J1401+5438	2.37	-27.4(-27.3)	14 01 48.40	54 38 59.0	...	...	<72	...	< 2.7[c]
J1837+5105	1.98	-29.3(-29.3)	18 37 25.30	51 05 59.0	...	...	<60	...	< 2.4[c]

[a]Priddey et al. 2002 detect this source at 350 GHz at 17.2± 2.9 mJy. At the time of submitting this paper no observations at 250GHz were made of this source.

[b]Priddey et al. 2002 detect this source at 350 GHz at 9.4± 2.8 mJy. At the time of submitting this paper no observations at 250GHz were made of this source.

[c]Omont et al. 2003

[d]Position derived from the Digital Sky Survey using AIPS program JMFIT

Note. — The source name is given in column [1], its redshift in [2], absolute blue magnitude (M_B) in [3], its optical position in J2000 coordinates

in [4], and [5]. The location of the 1.4 GHz radio emission peaks as derived from the Gaussian fitting is given in columns [6] and [7]. The flux densities at 1.4, 5 and 250 are given in in columns [8], [9], and [10] respectively with 1σ error bars. In cases of non-detections, 3 σ upper limits to flux densities are listed..

Table 2. Estimated Properties

QSO	L_{bol} $L_\odot$	${\alpha^5}_{1.4}$	$L_{1.4}$ W Hz^{-1}	$L_{5.0}$ W Hz^{-1}	L_{FIR} $L_\odot$	q
J0018-0220	2.20e+14	$\leq$ -0.61	8.3e+24	3.8e+24	2.3e+13	2.4 $\pm$ 0.2
J0035+4405	2.42e+14	$\leq$ -0.18	3.1e+24	2.5e+24	1.3e+13	2.3 $\pm$ 0.3
J0812+4028	6.07e+13	$\leq$ -0.60	2.7e+24	1.4e+24	1.7e+13	2.7 $\pm$ 0.4
J0937+7301	2.65e+14	0.15 $\pm$ 0.08	5.3e+24	6.4e+24	1.5e+13	2.4 $\pm$ 0.2
J1409+5628	2.42e+14	-0.90 $\pm$ 0.25	4.2e+25	1.4e+25	4.3e+13	2.0 $\pm$ 0.1
J1543+5359	2.20e+14	0.80 $\pm$ 0.20	7.2e+23	1.9e+24	1.6e+13	3.3 $\pm$ 0.3
J1611+4719	1.27e+14	$\leq$ -0.40	4.2e+24	2.5e+24	1.9e+13	2.5 $\pm$ 0.2
J1649+5303	1.83e+14	0.10 $\pm$ 0.30	8.9e+24	9.9e+24	1.9e+13	2.4 $\pm$ 0.2
J0837+145	1.83e+14	...	$\leq$ 3.0e+24	$\leq$ 1.1e+24	$\leq$ 7.3e+12	...
J0958+470	1.27e+14	...	$\leq$ 2.9e+24	$\leq$ 1.1e+24	$\leq$ 8.5e+12	...
J0914+582	6.66e+13	...	2.9e+24	9.6e+23	$\leq$ 7.3e+12	$\leq$ 2.5
J1210+3939	1.27e+14	...	2.5e+24	9.5e+23	$\leq$ 1.2e+13	$\leq$ 2.6
J1304+2953	1.67e+14	...	4.3e+24	1.7e+24	$\leq$ 1.2e+13	$\leq$ 2.5
J1309+2814	1.39e+14	...	$\leq$ 1.8e+24	$\leq$ 7.0e+23	$\leq$ 1.2e+13	...
J1401+5438	8.77e+13	...	$\leq$ 2.3e+24	$\leq$ 8.9e+23	$\leq$ 1.1e+13	...
J1837+5105	5.05e+14	...	$\leq$ 1.3e+24	$\leq$ 5.0e+23	$\leq$ 9.7e+13	...

Note. — Table 2 presents some of the estimated properties for the mm-detected sources (Column [1]). Their bolometric luminosities (Column [2]) were estimated from the absolute blue magnitudes given in Omont et al. (2003), using a WMAP cosmology. Omont et al. used the standard Einstein-de Sitter cosmology with $H_0 = 50$ km s^{-1} Mpc^{-1}, and $q_0 = 0.5$ to estimate the rest-frame absolute B band magnitudes, and so we scaled the blue magnitudes to the concordance cosmology by scaling the luminosity distances. To convert the blue luminosity L_B to a bolometric measurement L_{bol} we assumed a bolometric correction from the B band of $L_{bol}/L_B = 12$ (Elvis et al. 1994). The radio properties (1.4 GHz luminosity and 5 to 1.4 GHz spectral index, $\alpha^5_{1.4}$), the 1.4 and 5 GHz rest-frame luminosities are gvine in columns [3], [4] and [5]. For the objects observed at both 1.4 and 5 GHz we calculated the rest-frame 1.4 GHz luminosity using the estimated spectral indices, or the upper limits for the indices. For sources observed at only one radio frequency (1.4 GHz) we used a

default spectral index of -0.75. The FIR luminosity (column [6]) was derived assuming a dust temperature of 45 K, and an emissivity index $\beta = 1.5$. This translates to the following scaling: $L_{\rm FIR} \sim 4.7 \times 10^{12}$ $(\frac{S_{250}}{\rm mJy})$ $\rm L_\odot$ over the z range of interest. The q parameter is given in column [7].

Figure Captions

Figure 1: Images at 1.4 GHz of the sources detected at 1.4 GHz discussed in this paper. The FWHM of the Gaussian restoring beams are shown in the insets in all frames. Contour levels (solid lines) are a geometric progression in the square root of two starting at 2σ, with σ listed below (σ corresponds to the measured rms on the image). Three negative contours starting at -2σ (dashed) are included. The central cross in each image marks the optical QSO location.
Fig1a = J0018-0220, $\sigma = 17$ μJy beam^{-1}; Fig1b = J0035+4405, $\sigma = 16$ μJy beam^{-1}; Fig1c = J0812+4028, $\sigma = 27$ μJy beam^{-1}; Fig1d = J0937+7301, $\sigma = 21$ μJy beam^{-1}; Fig1e = J1409+5628, $\sigma = 23$ μJy beam^{-1}; Fig1f = J1543+5359, $\sigma = 19$ μJy beam^{-1}; Fig1g = J1611+4719, $\sigma = 19$ μJy beam^{-1} ; Fig1h = J1649+5303, $\sigma = 19$ μJy beam^{-1}; Fig1i = J0914+582, $\sigma = 30$ μJy beam^{-1}; Fig1j = J1210+3939, $\sigma = 25$ μJy beam^{-1}; Fig1k = J1304+2953, $\sigma = 22$ μJy beam^{-1};

Figure 2: Images at 4.8 GHz of the sources detected at this frequency. The FWHM of the Gaussian restoring beams are shown in the insets in all frames. Contour levels (solid lines) are a geometric progression in the square root of two starting at 2σ, with σ listed below (σ corresponds to the measured rms on the image). Two negative contours (dashed) are included. The central cross in each image marks the optical QSO location.
Fig1d = J0937+7301, $\sigma = \mu$Jy beam^{-1}; Fig1e = J1409+5628, $\sigma = \mu$Jy beam^{-1}; Fig1f = J1543+5359, $\sigma = \mu$Jy beam^{-1}; Fig1h = J1649+5303, $\sigma = \mu$Jy beam^{-1};

Figure 3: Radio(in W Hz^{-1}) versus mm luminosities (in $L_\odot$) for all our sources. The doted line represents the relation between 1.4 GHz and FIR luminosity for a star-forming object. This figure suggests that the mechanisms producing radio and mm emission in these quasars are connected. We note that flux density is not proportional with redshift so this tentative correlation cannot result from a mutual correlation with distance.

Figure 4: Distribution of q values plotted as a function of 60 μm luminosity. The crosses are for the IRAS 2Jy sample of Yun et al. (2001). The solid squares with error bars are for the mm-detected QSOs with steep radio spectral indices and the empty triangles are mm and radio detected source with almost flat or raising spectral indices (Table 2). The solid line marks the average value of $q = 2.34$, while the dotted lines mark the radio-excess (below) and IR-excess (above) objects, as discussed in Yun et al. (2001).

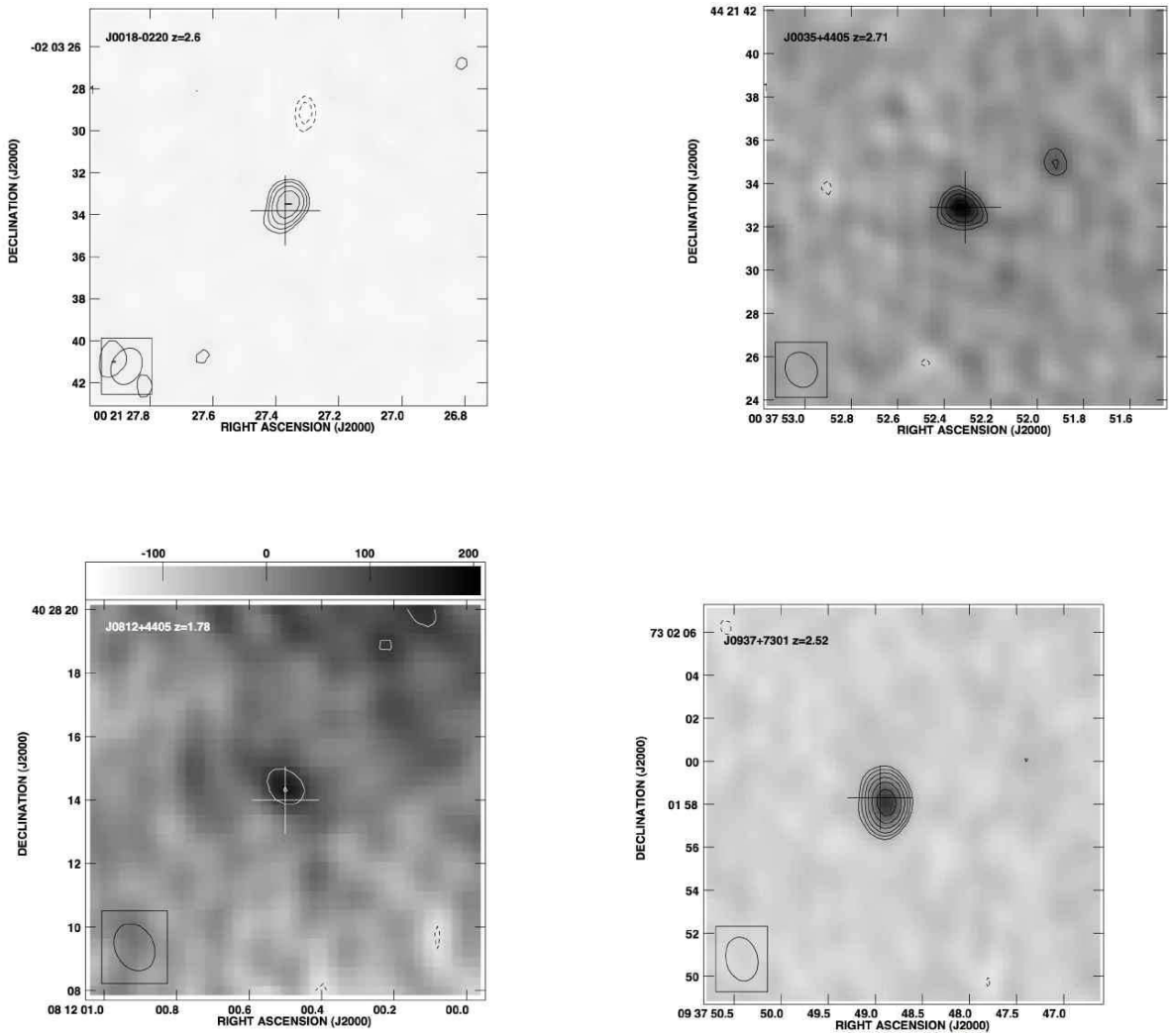

Fig. 1.— Images at 1.4 GHz

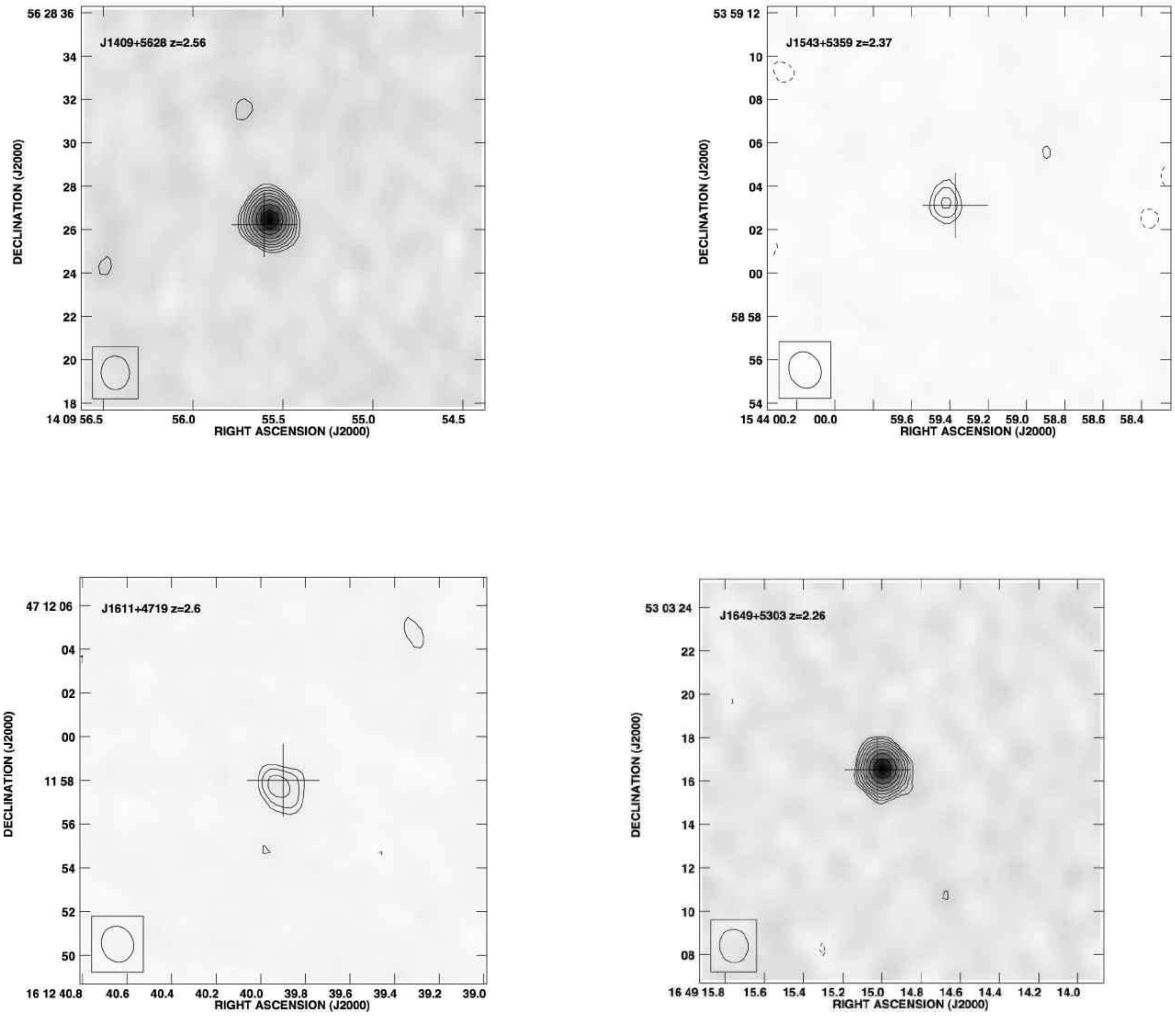

Fig. 1.— continued

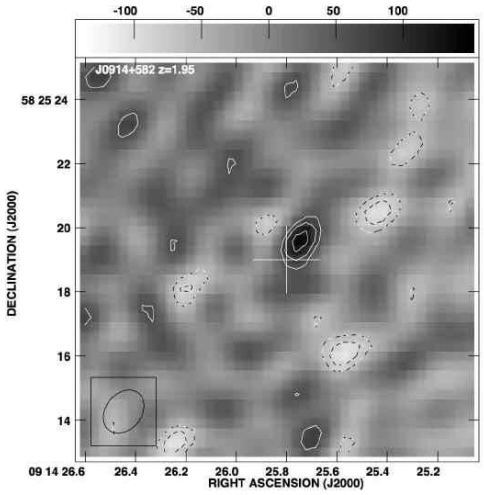
-100
-50
0
50
100
J0914+582 z=1.95
58 25 24
22
20
18
16
14
DECLINATION (J2000)
09 14 26.6
26.4
26.2
26.0
25.8
25.6
25.4
25.2
RIGHT ASCENSION (J2000)

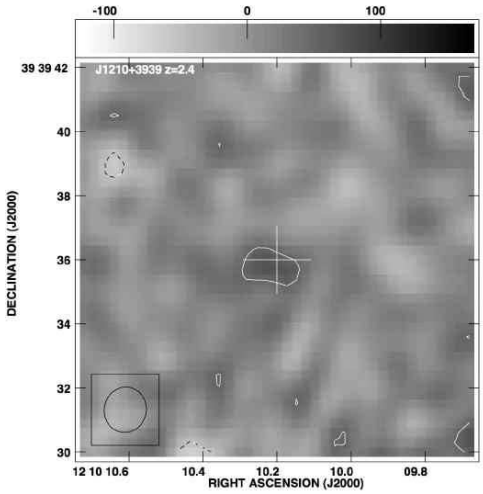
-100
0
100
J1210+3939 z=2.4
39 39 42
40
38
36
34
32
30
DECLINATION (J2000)
12 10 10.6
10.4
10.2
10.0
09.8
RIGHT ASCENSION (J2000)

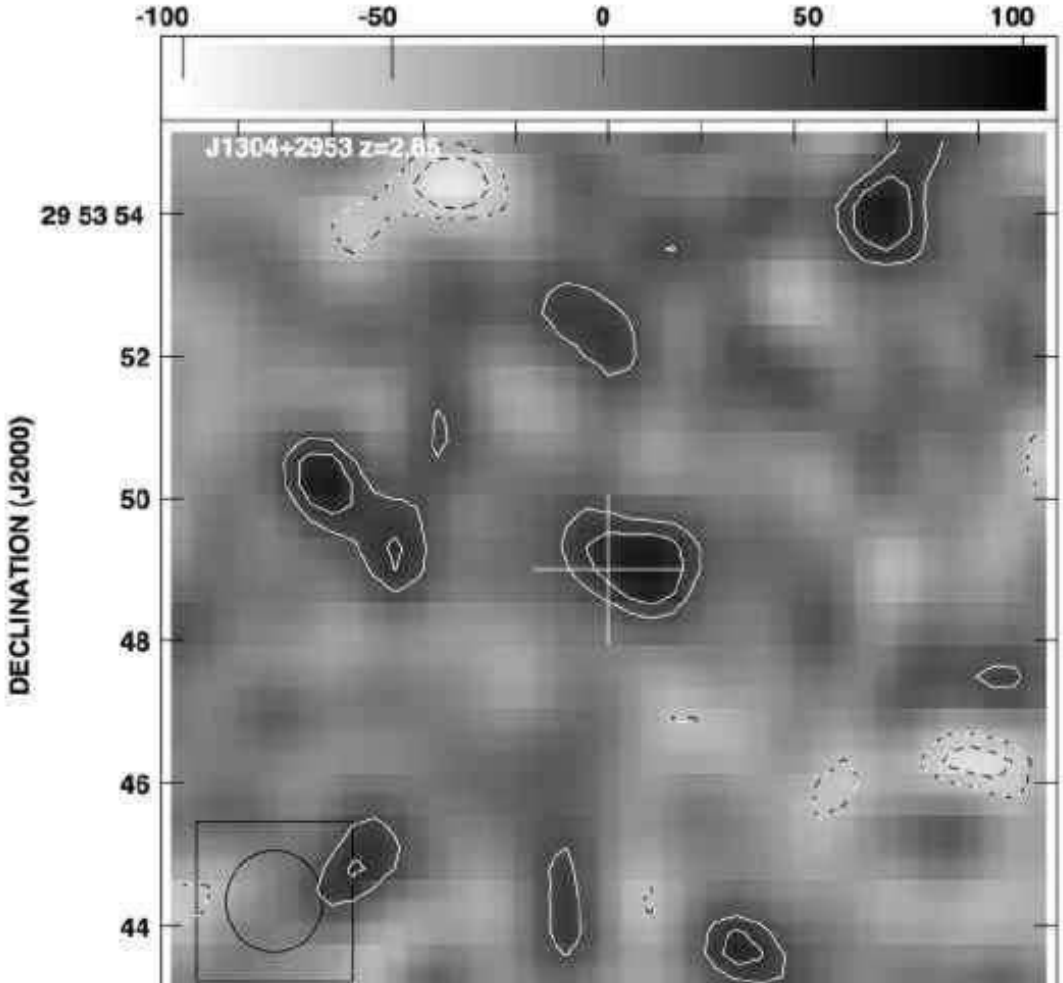
-100
-50
0
50
100
J1304+2953 z=2.85
29 53 54
52
50
48
46
44
DECLINATION (J2000)

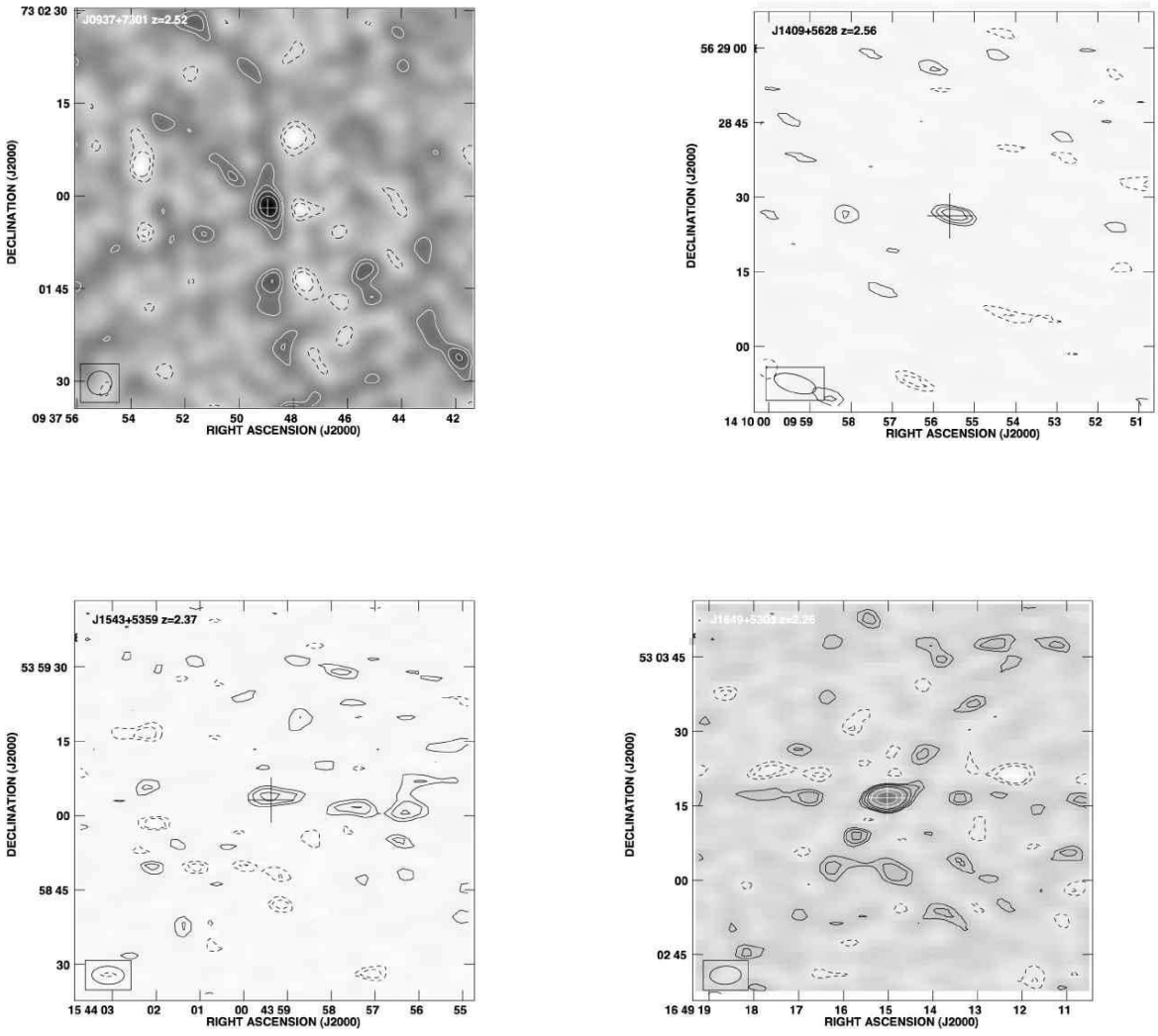

Fig. 2.— Images at 5 GHz

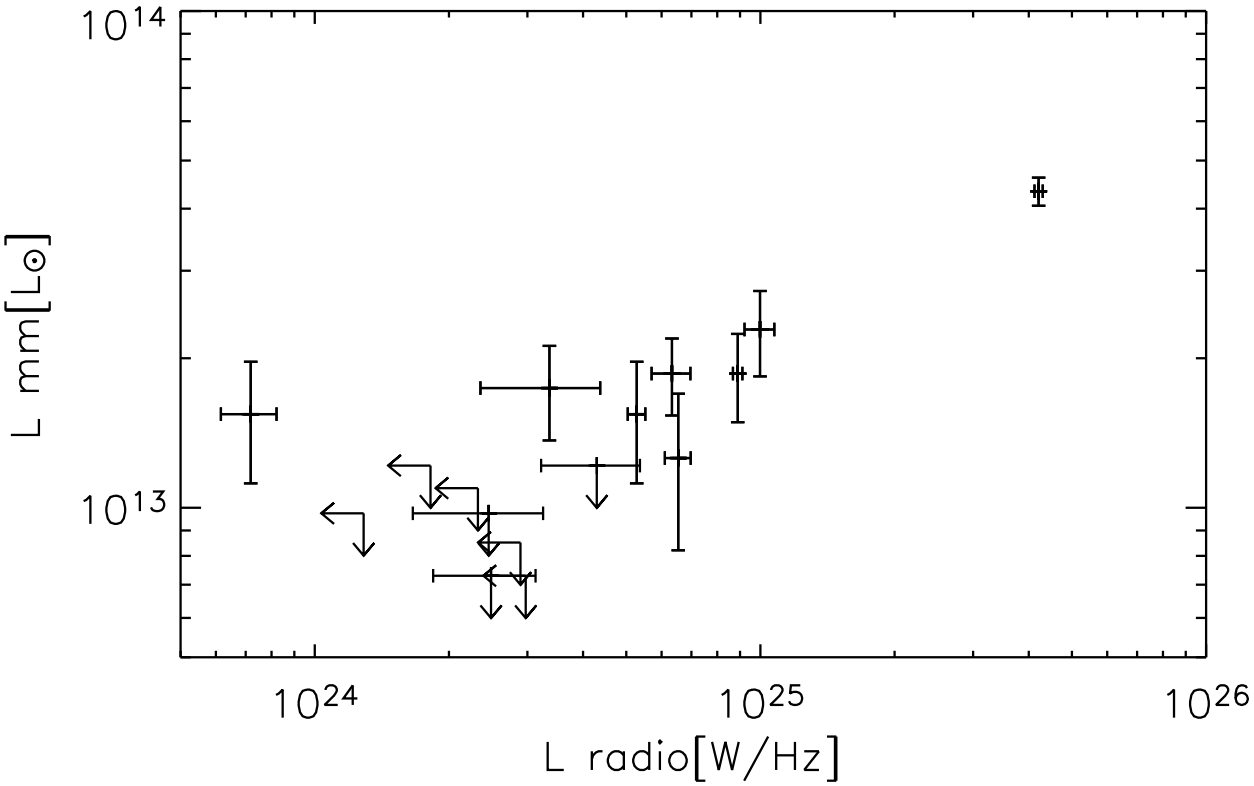
10^{14}
10^{13}
L mm[L⊙]
10^{24}
10^{25}
10^{26}
L radio[W/Hz]

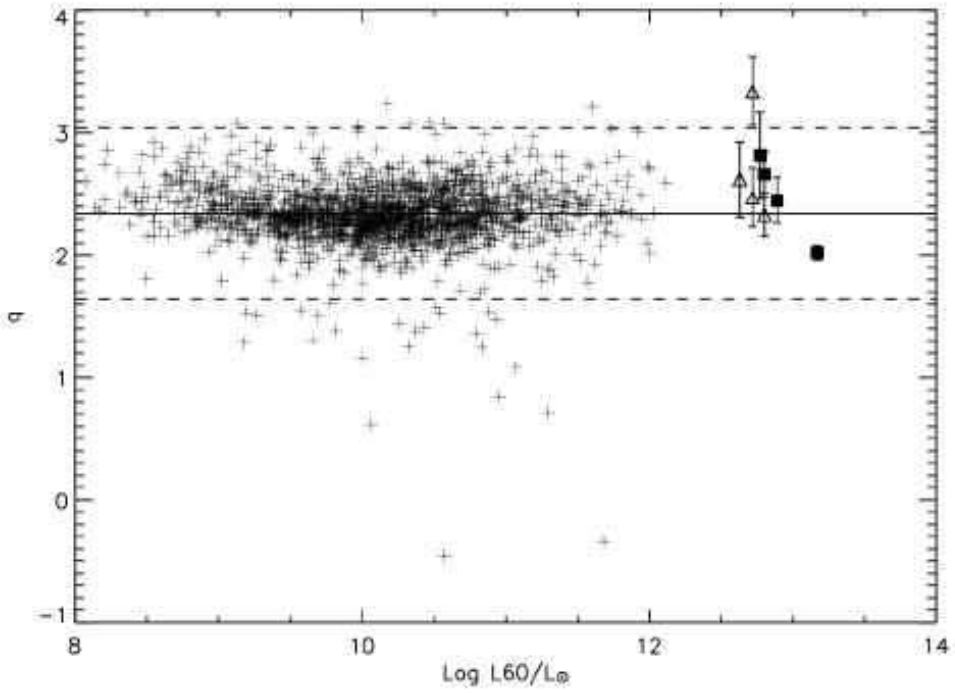
4
3
2
1
0
−1
q
8
10
12
14
Log L60/L⊙